6

Biomechanics and Modeling of Skeletal Soft Tissues

Rami K Korhonen[1] and Simo Saarakkala[2,3]
[1]*Department of Applied Physics, University of Eastern Finland, Kuopio*
[2]*Department of Medical Technology, University of Oulu, Oulu*
[3]*Department of Diagnostic Radiology*
University of Oulu and Oulu University Hospital, Oulu
Finland

1. Introduction

1.1 Articular cartilage

Articular cartilage is a specialized connective tissue that covers the ends of the bones in the diarthrodial joints. The thickness of human articular cartilage is typically between 1-6 mm. The main functions of articular cartilage are to dissipate and distribute contact stresses during joint loading, and to provide almost frictionless articulation in diarthrodial joints. In order to accomplish these demanding tasks, articular cartilage has unique mechanical properties. The tissue is a biphasic material with an anisotropic and nonlinear mechanical behaviour.

Articular cartilage is composed of two distinct phases. Fluid phase of the cartilage tissue consists of interstitial water and mobile ions. The water phase constitutes 68-85 % of the cartilage total weight and is an important determinant of the biomechanical properties of the tissue. Solid phase (or solid matrix) of the cartilage tissue consists mainly of collagen fibrils and negatively charged proteoglycans. The cell density is relatively small – in human adult tissue only ~2% of the total cartilage volume is occupied by the chondrocytes. Collagen molecules constitute 60-80% of the cartilage dry weight or approximately 10-20% of the wet weight. The collagen molecules assemble to form small fibrils and larger fibers that vary in organization and dimensions as a function of cartilage depth. The diameter of collagen fibers is approximately 20 nm in the superficial zone and 70-120 nm in the deep zone, and it varies between different collagen types. The collagen fibrils of the cartilage tissue consist mainly of type II collagen, although small amounts of other collagen types can be also found in cartilage, e.g. collagen type VI is common form in the vicinity of cells (pericellular matrix). In addition to the collagen fibrils, proteoglycan macromolecules constitute 20-40% of the cartilage dry weight or approximately 5-10% of the wet weight. The proteoglycan aggrecan is composed of a protein core and numerous glycosaminoglycan (GAG) chains attached to the core. Many aggrecan molecules are further bound to a single hyaluronan chain to form a proteoglycan aggregate.

The basic structure of the articular cartilage can be divided into four zones based on the arrangement of collagen fibril network (Benninghoff, 1925): 1) *Superficial zone*: here the

chondrocytes are flattened and aligned parallel to the cartilage surface. The collagen fibrils are relatively thin and run parallel to each other. The proteoglycan content is at its lowest and the water content is at its highest. 2) *Middle zone*: here the collagen fibrils have a larger diameter and they are oriented randomly. The cell density and water content is lower and proteoglycan content is higher than in the superficial zone. 3) *Deep zone*: here the diameter of the collagen fibrils is at its largest, and the collagen fibrils are oriented perpendicular to the articular surface. The cell density and water content are at their lowest, the proteoglycan content at its highest but the collagen content is variable. 4) *Calcified cartilage*: this thin layer is located between the deep zone and the subchondral bone and it joins the cartilage tissue to the subchondral bone. Here the chondrocytes usually express a hypertrophic phenotype.

It is nowadays widely accepted that collagen fibrils are primarily responsible for the cartilage tensile stiffness and the dynamic compressive stiffness. In contrast, proteoglycans are primarily responsible for the equilibrium properties during compression, and fluid contributes to the dynamic and time-dependent properties of the tissue. For more comprehensive description of structure-function relationships of cartilage, the reader may consult *e.g.* the book by Mow et al. (2005).

1.2 Meniscus

Meniscus is a wedge-shaped fibrocartilaginous structure between femoral and tibial articular cartilage surfaces inside the knee joint capsule. The function of the meniscus is to bear and dissipate loads, provide stability to the knee joint, and protect articular cartilage from excessive loads by functioning as a shock absorber. Similarly as in articular cartilage, meniscus has complex mechanical properties in order to accomplish these tasks.

Meniscus has also biphasic composition. Such as in cartilage, fluid phase of the meniscus consists of interstitial water and mobile ions. The water phase constitutes 60-70% of the meniscus total weight and is similarly important determinant of the biomechanical properties of the tissue. Solid phase of the meniscus consists of highly organized collagen fibril network, negatively charged proteoglycans and meniscal cells (fibrochondrocytes). Collagen molecules constitute 15-25 % of the meniscus wet weight. In contrast with articular cartilage, the collagen fibrils of meniscus consist mainly of type I collagen, *i.e.* also found in skin and bone tissues, although smaller amounts of types II, III, V, and VI can be also found in meniscus (McDevitt&Webber, 1990). Furthermore, meniscus contains significantly less proteoglycan than articular cartilage, only 1-2% of the wet weight.

The basic structure of meniscus can be divided into different layers based on the arrangement of the collagen fibril network. Since the meniscus is located between femoral and tibial articular surfaces, it has two surface layers both in top and bottom. Below surface layers are intermediate layers and in the center of the meniscus is the central layer. At the femoral surface layer the collagen fibrils are relatively thick and run parallel to each other and the femoral surface. In contrast, at the tibial surface layer the collagen fibrils are oriented randomly. At inner layers, the arrangement of collagen fibrils is more variable. The central layer can be further divided into four zones in the axial plane: anterior and posterior parts of the central layer exhibit relatively parallelly organized collagen fibrils, middle part of the central layer exhibits irregular organization medially, wheras organization changes

more regular and circular-shaped at the lateral side. For a more comprehensive and graphical description of structure and organization of collagen fibril network in the different layers of meniscus, the reader is recommended to consult the study of human meniscus structure by Cui&Min (2007).
Similarly as in cartilage, the collagen fibrils are mainly responsible for the tensile properties of meniscus and proteoglycans contribute strongly to the equilibrium response. Fluid has a significant role in carrying impact and dynamic loads. For more information of the general anatomical and functional properties of the meniscus, the reader may consult *e.g.* the review by Messner&Gao (1998).

1.3 Ligaments and tendons

Ligaments and tendons are soft tissues connecting bones to bones or bones to muscles, respectively. Their primary functions are to stabilize joints and transmit the loads, hold the joints together, guide the trajectory of bones, and control the joint motion area. Ligaments and tendons are also biphasic tissues having fluid and solid phases similarly as in articular cartilage and meniscus. Therefore, they also possess highly viscoelastic mechanical properties.
The fluid phase constitutes 60-70% of the total weight of ligaments and tendons. Solid phase consists of highly organized longitudinal collagen fibril network (over 15 % of the wet weight), elastin network, and proteoglycans. Similarly than in meniscus, the collagen fibrils of ligaments and tendons consist mainly of type I collagen. Since ligaments and tendons have so tightly packed and organized long collagen fibril network they have extremely high tensile strength and nonlinear stress-strain behavior.
For more information of the anatomical and functional properties of the ligaments and tendons, the reader may consult *e.g.* the book chapter by Woo et al. (2005).

	Collagen (wet weight)	**Proteoglycan (wet weight)**	**Fluid (wet weight)**	**Young's modulus**
Articular cartilage	10-20% (type II)	5-10%	68-85%	~0.5 MPa (compression)
Meniscus	15-25% (type I)	1-2%	60-70%	~0.1 MPa (compression)
Ligament	20-30% (type I)	less than in cartilage	60-70%	>100 MPa (tension)
Tendon	more than in ligament (type I)	less than in ligament	60-70%	>1000 MPa (tension)

Table 1. Main compositional parameters and elastic properties of articular cartilage, meniscus, ligaments and tendons.

2. Experimental mechanical characterization of skeletal soft tissues

2.1 Introduction

When skeletal soft tissues are mechanically tested, one can apply either force or deformation to it and then follow the other parameter. For example, constant or changing force may be

applied to a tissue and consequent change in the deformation is followed. Similarly, the change in force can be followed when constant or changing deformation is applied. Important parameter to describe the behavior of tissues under loading is strain (ε), defined as follows:

$$\epsilon = \frac{\Delta l}{l_0} \tag{2.1}$$

where Δl is the change in thickness/length of a tissue sample, and l_0 is the original thickness/length. The normalization with the original thickness/length ensures that the deformation is comparable between tissue samples with different thickness or length. It is important to note that, according to the definition, the strain is a unitless quantity.
Second important parameter in biomechanical testing is stress (σ), which is defined as:

$$\sigma = \frac{F}{A_0} \tag{2.2}$$

where F is the force applied to tissue, and A_0 is the original cross-sectional area in which the force is acting. Again here, the normalization with the cross-sectional area ensures that the load is comparable between different cross-sectional areas. The unit of stress is Pa, and the definition of stress is fundamentally the same as for pressure.
When both stress (σ) and strain (ε) are defined as above, mechanical behavior/properties of different skeletal soft tissues can be compared regardless of the size and shape of the samples. If the relation between stress and strain is assumed linear, one obtains the Hooke's linear model for solids from which the stiffness (elastic modulus) of the tissue can be calculated (see section 3.2).
When the compressive or tensile stress is applied to, say, excised soft tissue sample, consequent strain occurs in the direction of the loading. However, when the strain occurs in one direction in a three-dimensional soft tissue sample, there is always corresponding strain in the perpendicular direction. For example, when a soft tissue sample is stretched in one direction it typically simultaneously compresses in perpendicular direction changing its shape. The change of shape is the third important parameter in biomechanical testing. It is quantified with the parameter called the Poisson's ratio (ν), defined as follows:

$$\nu = -\frac{\varepsilon_{lat}}{\varepsilon} \tag{2.3}$$

where ε is the strain in loading direction and ε_{lat} is the corresponding strain in horizontal direction. The Poisson's ratio is the intrinsic parameter of a tissue, and it is unique for different materials. For example, an isotropic elastic material, e.g. rubber, has the Poisson's ratio of 0.5 in compression which means that the volume of the material does not change during mechanical loading. Since the major component of all human soft tissues is interstitial water, mechanical loading causes water to flow out of the tissue. Finally, after the complete relaxation, i.e. in equilibrium state, no fluid flow or pressure gradients exist in a tissue and, consequently, the entire stress is carried by the solid matrix. Because of this time-dependent viscoelastic nature, all human soft tissues have typically lower Poisson's ratios in compression than elastic materials, being in the range of 0.0 - 0.4 in

compression (Jurvelin et al., 1997; Korhonen et al., 2002a; Sweigart et al., 2004). On the other hand, Poisson's ratios in tension, shown for anisotropic materials, can be even more than 1 (Hewitt et al., 2001; Elliott et al., 2002).
It is also possible to apply load or deformation to a soft tissue sample parallel to the surface. This requires fixed contact between the tester and the surface of the sample. Then, so called shear strain (γ) is defined as follows:

$$\gamma = \frac{\Delta l_{shear}}{l_0} \tag{2.4}$$

where Δl_{shear} is the deformation of a surface point parallel to the surface, and l_0 is the sample thickness (perpendicular to the surface). Similarly, shear stress (τ) is defined as follows:

$$\tau = \frac{F_{shear}}{A_0} \tag{2.5}$$

where F_{shear} is the force applied parallel to the surface, and A_0 is the cross-sectional area of the contact between the tester and the surface of the sample.

2.2 Mechanical testing geometries

Mechanical testing geometries for soft tissues can be divided into compression, tension, bending and torsion. We will now consider only compression and tension since they are the most relevant geometries for skeletal soft tissues.
Compression testing is widely used especially for determination of mechanical properties of articular cartilage and meniscus. This is a relevant choice since also in vivo, e.g. during normal walking cycle, articular cartilage and meniscus experiences external compressive forces. When the tissue is mechanically tested in compression, three different measurement configurations can be used: unconfined compression, confined compression and indentation. In unconfined compression, a soft tissue sample is compressed between two smooth metallic plates to a predefined stress or strain. This geometry allows interstitial fluid flow out of the tissue only in the lateral direction (Fig. 1). In confined compression, a soft tissue sample is placed in a sealed chamber and, subsequently, compressed with a porous filter (Fig. 1). In this geometry the interstitial fluid can only flow axially through the tissue surface into the filter. In indentation geometry, a soft tissue is compressed with a cylindrical, typically plane-ended or spherical-ended indenter (Fig. 1). In this geometry, fluid flow outside the indenter-tissue contact point is possible in both the lateral and axial directions. It should be emphasized that the indentation is the only compressive geometry which is not limited into the laboratory use. Since indentation testing does not require a preparation of separate tissue samples it can be also performed in vivo. For example, stiffness of femoral articular cartilage has been measured during arthroscopy in vivo (Vasara et al., 2005).
Tensile testing is widely used especially for determination of mechanical properties of ligaments and tendons, while it is less used for the characterization of cartilage and meniscus properties. Again, this is a relevant choice for these tissues since they exhibit mainly tensile stresses in vivo. In tensile testing, a soft tissue sample is fixed with two ends, e.g. by using metallic clamps, and the sample is then streched to a predefined stress or strain.

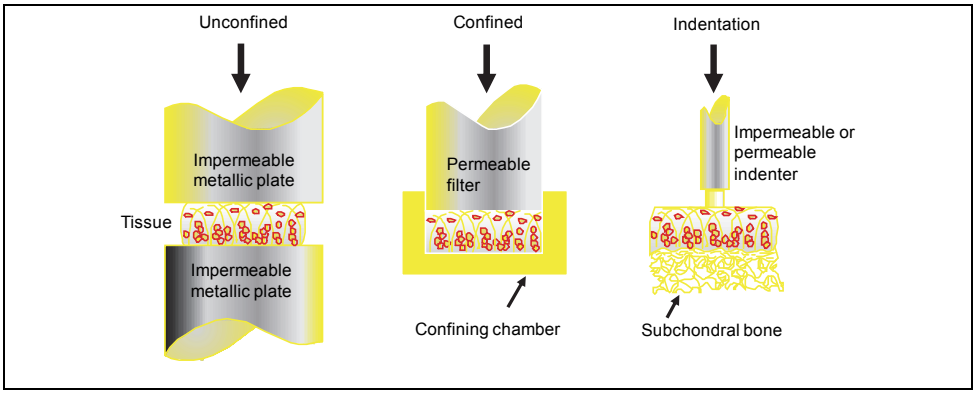

Fig. 1. Unconfined, confined and indentation loading geometries for testing of mechanical properties of articular cartilage.

2.3 Destructive and nondestructive testing protocols

In all experimental mechanical testing geometries it is possible to conduct both destructive and non-destructive testing. In non-destructive protocol tissue is tested with small strains or loads and all the changes induced to the tissue are reversible. In contrast, destructive protocol involves larger strains or loads inducing non-reversible changes to a tissue.

Most common non-destructive testing protocols are called creep and stress-relaxation. These tests can be conducted both in compression and tension geometries. In creep test, constant compressive or tensile stress is applied to a tissue and corresponding strain is followed as a function of time (Fig. 2). In stress-relaxation test, predefined compressive or tensile strain is applied and corresponding stress is followed as a function of time (Fig. 2). All biphasic and viscoelastic soft tissues exhibit first the relaxation phase in both testing protocols, and finally when the tissue reaches its equilibrium state, no fluid flow or pressure gradients exist. Consequently, after the relaxation phase, strain (in creep test) or stress (in stress-relaxation test) stabilizes at the constant level, and then the entire load is carried by the solid matrix of a tissue.

Destructive testing is typically conducted for skeletal soft tissues only in tension geometry. Then it is common to follow the tissue mechanical behaviour from the stress-strain curve. At the beginning phase of tension test of skeletal soft tissue, one can observe so called toe region (Fig. 3). In this region, the relation between stress and strain is nonlinear and the slope is increasing with increased loading. The reason for the increasing slope is the straightening of the wavy-like collagen fibrils. After the collagen fibrils are completely straightened begins the elastic region (Fig. 3). In this region, the stress and strain are linearly related and the slope of the curve is called the Young's modulus of tissue. In the elastic range, all changes of a tissue are still reversible, i.e. if the stress is removed tissue returns to the original strain. All non-destructive tests, such as creep and stress-relaxation tests mentioned above, should be conducted in this elastic region. It should be also noted that in human skeletal soft tissues the loading rate affects the slope of the elastic range, i.e. higher loading rate results to steeper slope and higher Young's modulus value.

When the stress is further increased from the elastic region, the slope of the curve changes and the plastic region begins. This is called the yield point (Fig. 3). After the yield point tissue begins to experience destructive changes, e.g. microfractures in the collagen fibril network. In the plastic region irreversible changes have occurred in a tissue and it does not

return to the original strain although the stress would be completely removed. The yield point is one typical parameter reported for soft tissues under destructive testing.
After the plastic region, the sudden failure of the tissue occurs and stress disappears (Fig. 3). The location of the breakdown is called the failure point, which is one typical parameter reported for soft tissues under destructive tensile testing.

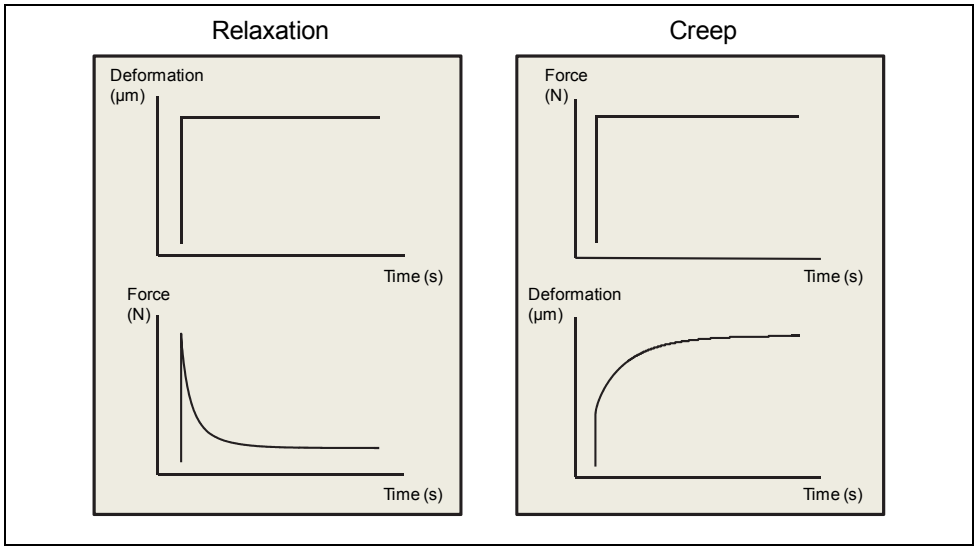

Fig. 2. Stress-relaxation (left) and creep (right) testing protocols.

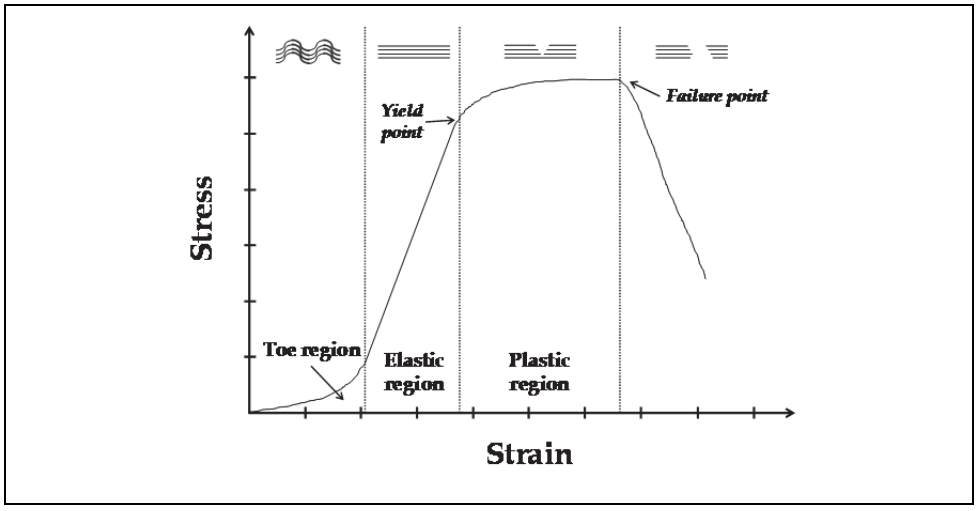

Fig. 3. Typical stress-strain curve for destructive tensile testing of skeletal soft tissues. Collagen fibril straightening and failure, related to different regions of the stress-strain curve, are also schematically shown.

3. Biomechanical modeling of skeletal soft tissues

3.1 Introduction

In this section, we will present the development of computational models applied for the characterization of biomechanical properties of cartilage, meniscus, ligaments and tendons. We will start from traditional linearly elastic models that can be applied for the characterization of static or dynamic properties of tissues by a simple Hookean relation. As the linear elastic model is only applicable for small strains, we will also introduce hyperelastic models that can be applied for nonlinear problems in larger strains.
Second, we will show traditional solid viscoelastic models, i.e. Maxwell, Voigt and Kelvin models. We will show the basic equations of these models. Then, we will take fluid into account in the model and present a biphasic, poroelastic model. We will present biphasic models with isotropic and anisotropic solid matrixes, improving the prediction of experimentally found mechanical behavior of fluid-saturated soft tissues.
Finally, we will present the fibril reinforced biphasic model of cartilage. In this model, the solid matrix is divided into fibrillar and non-fibrillar parts. We will also present different forms of nonlinearities formulated especially for the collagen fibers and the swelling properties due to the fixed charge density of proteoglycans. At the end of the section, we will summarize the application of the presented constitutive models for cartilage, menisci, ligaments and tendons.

3.2 Linear elastic model

The most traditional and simplest mechanical model for skeletal soft tissues is Hooke's linear elastic model for solid materials. This model assumes the linear relation between stress and strain, corresponding to a spring fixed from one end and compressed or strecthed from the other. Hooke's model can be presented as follows:

$$\sigma = E\epsilon, \tag{3.1}$$

where σ is stress, ε is strain, and E is the elastic (Young's) modulus: This model is easy to apply for various testing geometries and protocols, and consequently stiffness of a tested soft tissue can be expressed by the Young's modulus. However, it should be realized that this simple model is limited to one-dimensional geometry and it assumes tissue as elastic and isotropic material. Hooke's law can be generalized to three-dimensional geometry and then also the Poisson's ratio (ν) is needed to describe the mechanical behaviour of the tested soft tissue (see section 3.5.1). Obviously, this is still not adequate for viscoelastic and anisotropic skeletal soft tissues.
Hooke's law can be further generalized for an anisotropic elastic material, when it can be expressed as a matrix form:

$$[\sigma] = [C][\epsilon], \tag{3.2}$$

where $[\sigma]$ is the stress tensor, $[\varepsilon]$ is the strain tensor, and $[C]$ is the stiffness matrix. In order to completely characterize the mechanical behaviour of anisotropic and elastic tissue, altogether 21 stiffness components are needed in $[C]$. For the material with mutually perpendicular planes of elastic symmetry, i.e. orthotropic material, nine elastic constants are needed in $[C]$. Furthermore, if one assumes the same mechanical properties in one plane (e.g. in x–y plane) and different properties in the direction normal to this plane (e.g. z-axis), five independent elastic constants are needed in $[C]$ and the material is referred as transversely isotropic (see section 3.5.2).

Even though one could determine all required stiffness components for an anisotropic elastic material, the mechanical behaviour of skeletal soft tissues still cannot be described by this linear model. In general, the linear elastic model can be applied for skeletal soft tissues when strains are small and the stress-strain relationship can be assumed linear. However, many soft tissues experience large strains in vivo. Furthermore, time-dependent behaviour (due to viscoelasticity) and different mechanical responses in compression and tension, both typical to skeletal soft tissues, cannot be described with this simple model. Therefore, more sophisticated models are needed for the mechanical characterization of skeletal soft tissues.

3.3 Hyperelastic model

Many biological tissues experience large deformations and then the stress-strain relationship becomes nonlinear. These materials are called hyperelastic materials. There are several hyperelastic material models developed, e.g. Neo-Hookean, Arruda-Boyce, Mooney-Rivlin, Ogden models. We will present here one of these models (Neo-Hookean model) that has been typically applied for many biological soft tissues.

The Neo-Hookean material model uses a general strain energy potential for finite strains:

$$U = C_1(\overline{I_1} - 3) + \frac{1}{D_1}(J_{el} - 1)^2, \tag{3.3}$$

where C_1 and D_1 are material parameters, J_{el} is the elastic volume ratio and $\overline{I_1}$ is the first deviatoric strain invariant defined as:

$$\overline{I_1} = \overline{\lambda_1}^2 + \overline{\lambda_2}^2 + \overline{\lambda_3}^2, \tag{3.4}$$

where $\bar{\lambda}_i = J^{-\frac{1}{3}}\lambda_i$ are the deviatoric stretches, J is is the total volume ratio, and λ_i are the principal stretches. The material parameters are given by:

$$C_1 = \frac{G_0}{2}, \quad D_1 = \frac{3(1-2\nu)}{G_0(1+\nu)} \tag{3.5}$$

where G_0 is the initial shear modulus and v is the Poisson's ratio. For linear elastic materials, the shear modulus can be expressed with the Young's modulus ($E = 2G_0(1+\nu)$).

3.4 Viscoelastic models

There are three typical viscoelastic solid materials that have been applied for biological soft tissues; Maxwell, Voigt and Kelvin (Standard linear solid) (Fig. 4). In contrast to the elastic or hyperelastic materials, these models have a time-dependent component that enables the modelling of creep, stress-relaxation and hysteresis.

The solid voscoelastic models are composed of elastic and viscous components. The elastic component is that shown in eq. 3.1, while the viscous component (dashpot) is velocity dependent as:

$$F = \eta \frac{dx}{dt} \tag{3.6}$$

where η is the damping coefficient, F is force and x is deformation/elongation. F and x can also be replaced with stress (σ) and strain (ε). In the Maxwell model, both the spring and dashpot experience the same force, while their deformation and velocity are different. The total velocity becomes:

$$\frac{dx}{dt} = \frac{1}{\mu}\frac{dF}{dt} + \frac{F}{\eta} \tag{3.7}$$

In the Voigt model, the forces of the spring and dashpot elements are different, but their deformation is the same. Thus, the total force is the sum of forces acting on the spring and dashpot:

$$F = \mu x + \eta \frac{dx}{dt} \tag{3.8}$$

In the Kelvin model, the combination of two springs and one dashpot complicates the equation of motion. The same principles as with the Maxwell and Voigt models can be applied, i.e. the elements that are side by side, undergo the same deformation but different force, while those that are arranged consecutively, experience the same force but different deformation. Subsequently, it can be proven that the equation of motion becomes:

$$F + \tau_\epsilon \frac{dF}{dt} = E_R \left(x + \tau_\sigma \frac{dx}{dt} \right) \tag{3.9}$$

where

$$\tau_\epsilon = \frac{\eta_1}{\mu_1}, \tau_\sigma = \frac{\eta_1}{\mu_0}\left(1 + \frac{\mu_0}{\mu_1}\right), E_R = \mu_0. \tag{3.10}$$

There are several textbooks that derive creep and stress-relaxation equations of the aforementioned viscoelastic models. See for instance Fung (2004).

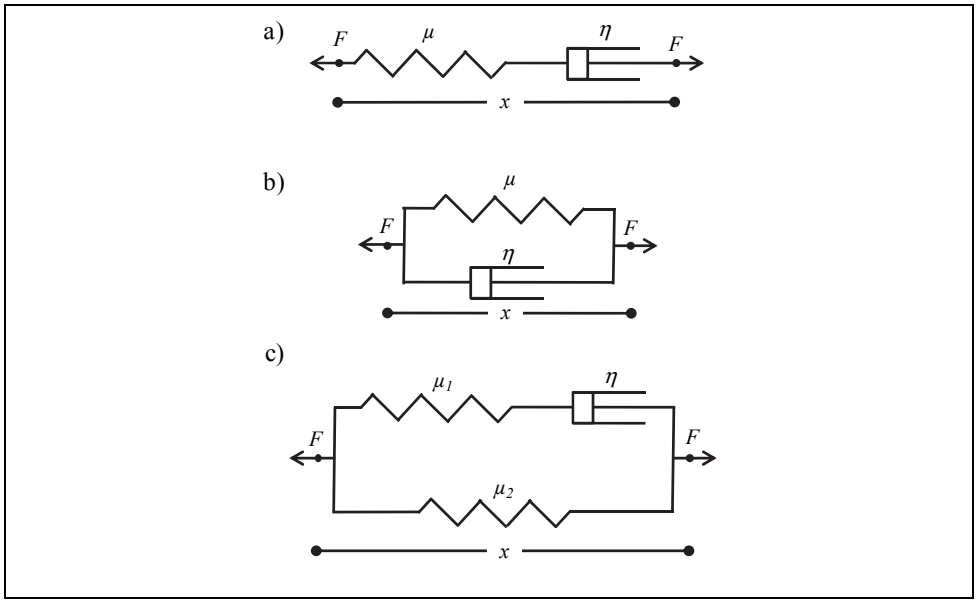

Fig. 4. Solid viscoelastic models: a) Maxwell, b) Voigt, c) Kelvin. F=force, μ=spring constant, η=damping coefficient, x=distance.

3.5 Biphasic, poroelastic model

The biphasic model is the most traditional model of articular cartilage and other fluid-saturated tissue which takes the interstitial fluid movement into account (Mow et al., 1980). In the biphasic theory, the solid matrix and fluid are assumed to be intrinsically incompressible and nondissipative. The only dissipative factor is the fluid flow in the tissue. The constitutive equations, i.e, the stress-strain relations for the solid, fluid and entire tissue are given by:

$$\boldsymbol{\sigma_s} = -\phi_s p\boldsymbol{I} + \boldsymbol{\sigma_E}, \tag{3.11}$$

$$\boldsymbol{\sigma_f} = -\phi_f p\boldsymbol{I}, \tag{3.12}$$

$$\boldsymbol{\sigma_t} = \boldsymbol{\sigma_s} + \boldsymbol{\sigma_f} = -p\boldsymbol{I} + \boldsymbol{\sigma_E}, \tag{3.13}$$

where $\boldsymbol{\sigma_s}$, $\boldsymbol{\sigma_f}$ and $\boldsymbol{\sigma_t}$ are solid, fluid and total stress tensors, respectively, ϕ_s and ϕ_f are volume fractions for the solid and fluid, respectively, p is the fluid pressure, $\boldsymbol{I}$ is the unit tensor and $\boldsymbol{\sigma_E}$ is the effective solid stress tensor.

For the biphasic material with linearly elastic Hookean solid matrix (see eqs. 3.1 and 3.2), the effective solid stress can be written as follows:

$$\boldsymbol{\sigma_E} = \boldsymbol{C\epsilon}, \tag{3.14}$$

where $\boldsymbol{C}$ is the stiffness matrix and $\boldsymbol{\epsilon}$ is the elastic strain tensor. The effective solid stress tensor alone resists the deformation at equilibrium, when the fluid flow has ceased.

With both solid and fluid phases considered intrinsically incompressible and homogenous, the balance of mass (continuity equation) is given by:

$$\boldsymbol{\nabla} \cdot (\phi_s \boldsymbol{v_s} + \phi_f \boldsymbol{v_f}) = \boldsymbol{0}, \tag{3.15}$$

where $\boldsymbol{v_s}$and $\boldsymbol{v_f}$ are velocity vectors of the solid and fluid phases. Neglecting inertia effects (acceleration = 0), the momentum equations for the solid and fluid phases are:

$$\boldsymbol{\nabla} \cdot \boldsymbol{\sigma_\alpha} + \boldsymbol{\pi_\alpha} = \boldsymbol{0}, \tag{3.16}$$

$$\boldsymbol{\pi_s} = -\boldsymbol{\pi_f} = \frac{\phi_f^2}{k}(\boldsymbol{v_f} - \boldsymbol{v_s}) \tag{3.17}$$

$$\boldsymbol{\nabla} \cdot \boldsymbol{\sigma_t} = \boldsymbol{0}, \tag{3.18}$$

where permeability k is related to the diffusive drag coefficient K by:

$$k = \frac{\phi_f^2}{K}. \tag{3.19}$$

The permeability k can be defined to be dependent on the porosity and void ratio, i.e. ratio of fluid to solid content, according to the following equation:

$$k = k_0 \left(\frac{1+e}{1+e_0}\right)^M, \tag{3.20}$$

where k_0 is the initial permeability, e_0 and e are initial and current void ratios, and M is a positive constant. The void ratio or fluid fraction has also been modeled in a depth-dependent manner, e.g,

$$\phi_f = 0.80 - 0.10\text{z}, \tag{3.21}$$

where z is the tissue depth (0: cartilage surface, 1:cartilage-bone interface).

3.5.1 Isotropic model

The elastic parameters of the biphasic poroelastic tissue can be obtained from the equation 3.14. The simplest form of linear elasticity is the isotropic case. The stress-strain relationship becomes:

$$\boldsymbol{\sigma_E} = \frac{E}{(1+\nu)(1-2\nu)} \begin{bmatrix} 1-\nu & \nu & \nu & 0 & 0 & 0 \\ \nu & 1-\nu & \nu & 0 & 0 & 0 \\ \nu & \nu & 1-\nu & 0 & 0 & 0 \\ 0 & 0 & 0 & 1-2\nu & 0 & 0 \\ 0 & 0 & 0 & 0 & 1-2\nu & 0 \\ 0 & 0 & 0 & 0 & 0 & 1-2\nu \end{bmatrix} \boldsymbol{\epsilon}. \tag{3.22}$$

Subsequently, the isotropic biphasic or poroelastic model consists of three material parameters: elastic parameters (Young's modulus (E), Poisson's ratio (ν)) and permeability (k, eq. 3.19)).

The biphasic isotropic material is equivalent to the elastic isotropic material at equilibrium and under dynamic loading. In these representations, it is assumed that at equilibrium all fluid flow has ceased and that the instantaneous response ($t \rightarrow 0$) of the biphasic tissue corresponds to that of an incompressible elastic material (ν = 0.5). These elastic isotropic models are useful if one wishes to obtain simple material parameters for the tissue. However, a more detailed description of the complex mechanical properties of skeletal soft tissues can only be obtained by using more sophisticated models.

3.5.2 Transversely isotropic model

In the transversely isotropic material, the mechanical parameters depend on the three mutually orthogonal directions. However, the properties are considered isotropic in the x-y plane. Then, the stiffness matrix relates the stress and strain tensors as follows:

$$\boldsymbol{\sigma_E} = \begin{bmatrix} \frac{1-\nu_{pz}\nu_{zp}}{E_p E_z \Delta} & \frac{\nu_p + \nu_{zp}\nu_{pz}}{E_p E_z \Delta} & \frac{\nu_{zp} + \nu_p \nu_{zp}}{E_p E_z \Delta} & 0 & 0 & 0 \\ \frac{\nu_p + \nu_{pz}\nu_{zp}}{E_z E_p \Delta} & \frac{1-\nu_{zp}\nu_{pz}}{E_z E_p \Delta} & \frac{\nu_{zp} + \nu_{zp}\nu_p}{E_z E_p \Delta} & 0 & 0 & 0 \\ \frac{\nu_{pz} + \nu_p \nu_{pz}}{E_p^2 \Delta} & \frac{\nu_{pz}(1+\nu_p)}{E_p^2 \Delta} & \frac{1-\nu_p^2}{E_p^2 \Delta} & 0 & 0 & 0 \\ 0 & 0 & 0 & 2G_{zp} & 0 & 0 \\ 0 & 0 & 0 & 0 & 2G_{zp} & 0 \\ 0 & 0 & 0 & 0 & 0 & \frac{E_p}{1+\nu_p} \end{bmatrix} \boldsymbol{\epsilon}, \tag{3.23}$$

where

$$\Delta = \frac{(1+\nu_p)(1-\nu_p-2\nu_{pz}\nu_{zp})}{E_p^2 E_z}. \tag{3.24}$$

The total number of transversely isotropic biphasic poroelastic parameters can now be written in terms of the Young's modulus and Poisson's ratio in the transverse plane, i.e. parallel to the articular surface (E_p and ν_p), out-of-plane Young's modulus and Poisson's ratio (E_{pz} and ν_{pz}), out-of-plane shear modulus (G_{zp}), and permeability (k, eq. 3.19).
Under an instantaneous loading ($t \to 0$), when fluid is entrapped in the tissue, the transversely isotropic biphasic or poroelastic material behaves like an incompressible elastic material (Garcia et al., 2000; Korhonen et al., 2002b), similarly as in the case of the isotropic model. The elastic parameters are then:

$$E_{pz}, E_p, \nu_{pz} = 0.5, \nu_p = 1 - 0.5\frac{E_p}{E_{pz}}, G_{zp}. \tag{3.25}$$

Similarly at equilibrium, when the fluid flow has ceased and only the solid matrix resists the compression, the material can be assumed to be elastic with the five independent material parameters in eq. 3.23.

3.5.3 Fibril reinforced model

In the fibril reinforced biphasic model, the fibril network (collagen network), in addition to the isotropic biphasic matrix, contributes to the mechanical response of tissues under loading (Korhonen et al. 2003). Thus, the total stress becomes:

$$\boldsymbol{\sigma_t} = \boldsymbol{\sigma_{nf}} + \boldsymbol{\sigma_{fibril}} - p\boldsymbol{I}, \tag{3.26}$$

where $\boldsymbol{\sigma_{nf}}$ and $\boldsymbol{\sigma_{fibril}}$ are nonfibrillar and fibril network stresses, respectively. The isotropic biphasic nonfibrillar matrix has been modeled as Hookean or Neo-Hookean materials with Darcy's law for the fluid flow (sections 3.2 and 3.3). The material parameters for the nonfibrillar part are the Young's modulus (E_m), Poisson's ratio (ν_m) and permeability (k). The fibril network properties are controlled by the Young's modulus of the fibril network (E_f). Elastic properties of the fibril network have been characterized with a nonlinear relation:

$$E_f = E_f^0 + E_f^\epsilon \epsilon_f, \text{for } \epsilon_f > 0, \tag{3.27}$$

$$E_f = 0, \text{for } \epsilon_f \leq 0, \tag{3.28}$$

where E_f^0 is the initial fibril network modulus, E_f^ϵ is the strain-dependent fibril network modulus, and ϵ_f is the fibril strain. The significant difference between the fibril reinforced and transversely isotropic poroelastic model is that the fibrils in the fibril reinforced model resist only tension, whereas E_p in the transversely isotropic model is the same for both compression and tension.
The collagen fibril stresses (σ_f) have also been modeled as viscoelastic:

$$\sigma_f = -\frac{\eta}{2\sqrt{(\sigma_f - E_f^0\varepsilon_f)E_f^\varepsilon}}\dot{\sigma_f} + E_f^0\varepsilon_f + \left(\frac{\eta E_f^0}{2\sqrt{(\sigma_f - E_f^0\varepsilon_f)E_f^\varepsilon}} + \eta\right)\dot{\varepsilon_f}, \text{for } \varepsilon_f > 0, \tag{3.29}$$

$$\sigma_f = 0, \text{for } \varepsilon_f \leq 0,$$

where η is the viscoelastic damping coefficient, and $\dot{\varepsilon}$ and $\dot{\sigma}$ are the stress- and strain-rates, respectively.

The fibrillar part has also been modeled with primary and secondary fibrils (Wilson et al., 2004). The primary fibrils represent the collagens detected with polarized light microscopy (Arokoski et al., 1996; Korhonen et al., 2002b), which cause a depth-dependent tensile modulus for the tissue. The fibrils are oriented vertically in the deep zone, curve in the middle zone, and reach a parallel orientation with the articular surface in the superficial zone (Benninghoff, 1925). Two parameters are needed to describe the fibril orientation: thickness of the superficial zone (d_{vec}) and bending radius of the collagen fibrils in the middle zone (r_{vec}). The secondary fibrils mimic the less organized collagen network which are observed in scanning electron microscopy (Kaab et al., 2003). The stresses for primary and secondary fibrils can be formulated as:

$$\sigma_{f,p} = \rho_z C \sigma_f, \tag{3.30}$$

$$\sigma_{f,s} = \rho_z \sigma_f, \tag{3.31}$$

where ρ_z represents the depth dependent fibril density, and C is the density ratio of primary and secondary fibrils. The stress of the fibril network is then determined as the sum of the stresses in each individual fibril ($\sigma_{f,all}^i$),

$$\sigma_f = \sum_{i=1}^{totf} \sigma_{f,all}^i. \tag{3.32}$$

3.5.4 Other models of skeletal soft tissues

There are also other models of biological soft tissues than those presented above. The conewise linear elastic model is able to characterize compression-tension nonlinearity of the tissues (Soltz&Ateshian, 2000). The poroviscoelastic model includes both fluid flow dependent and fluid flow independent viscoelasticities (DiSilvestro&Suh, 2001). The triphasic model includes ion flow (Lai et al., 1991) and it is equivalent to the biphasic swelling model at equilibrium (Wilson et al., 2005a). In the biphasic fibril reinforced swelling model, after inclusion of osmotic swelling and chemical expansion, the total stress becomes:

$$\boldsymbol{\sigma_t} = \boldsymbol{\sigma_{nf}} + \boldsymbol{\sigma_{fibril}} - \Delta\pi \boldsymbol{I} - T_c \boldsymbol{I} - \mu_f \boldsymbol{I}, \tag{3.33}$$

where $\Delta\pi$ is the osmotic pressure gradient, T_c is the chemical expansion stress, and $\mu_f = p - \Delta\pi$ is the chemical potential of fluid (Huyghe&Janssen, 1997; Wilson et al., 2005a; Wilson et al., 2005b; Korhonen et al., 2008). The osmotic pressure gradient is caused by the difference in ion concentration of the cartilage and that of the surrounding fluid (Huyghe&Janssen, 1997; Wilson et al., 2005a; Wilson et al., 2005b). It is also referred to as the Donnan swelling pressure gradient. The chemical expansion stress comes from the repulsion between negative charges in the solid matrix (Lai et al., 1991; Wilson et al., 2005a; Wilson et al., 2005b). Swelling of the tissue is resisted by the collagen network, inducing pre-stresses in the collagen fibrils. This model has been applied specifically for cartilage since its swelling properties due to the fixed charge density have a significant role for the deformation behavior of the tissue, especially under static loading. For the

implementation of swelling properties, the fixed charge density can be taken from experimental measurements (Maroudas, 1968; Chen et al., 2001).
Other anisotropic and nonlinear representation have also been presented for biological soft tissues. Specifically the collagen fibrils and their nonlinear stress-strain tensile behavior has been presented as follows:

$$P_1 = E_1(e^{k_1\varepsilon_f} - 1), \tag{3.34}$$

$$P_2 = E_2(e^{k_2\varepsilon_e} - 1), \tag{3.35}$$

$$P_f = P_1 + P_2, \tag{3.36}$$

where P_f is the first Piola-Kirchhoff fibril stress, ε_f is the total fibril strain, ε_e is the strain of the spring μ_1 (Fig. 3c), and E_1, E_2, k_1 and k_2 are constants (Wilson et al., 2006; Julkunen et al., 2008). Tensile stress-stretch relationship for collagen fibrils has also been presented in the following form

$$\lambda\frac{\partial F_2}{\partial\lambda} = \begin{cases} 0, & \lambda < 1, \\ C_3\left(e^{C_4(\lambda-1)} - 1\right) & 1 < \lambda < \lambda^*, \\ C_5\lambda + C_6 & \lambda > \lambda^*, \end{cases} \tag{3.37}$$

where

$$C_6 = C_3\left(e^{C_4(\lambda^*-1)} - 1\right) - C_5\lambda^*. \tag{3.38}$$

In these equations, F_2 is the strain energy function for the collagen fibers, usually in conjunction with the hyperelastic model, such as Neo-Hookean (eq. 3.3), λ is fiber stretch, λ^* is the stretch where collagen fibers are straightened, and C_3, C_4, C_5 and C_6 are material constants (Pena et al., 2006; Zhang et al., 2008).

3.6 Models applied for skeletal soft tissues

Articular cartilage has been modelled using almost all the above mentioned models (Mow et al., 1980; Lai et al., 1991; Li et al., 1999; Garcia et al., 2000; Guilak&Mow, 2000; Soltz&Ateshian, 2000; DiSilvestro&Suh, 2001; Korhonen et al., 2003; Laasanen et al., 2003; Wilson et al., 2004; Julkunen et al., 2007). The choice of the material model has been mainly based on the study purpose and loading protocol. Recently, however, the fibril reinforced material description has been applied by many researchers and it is probably the most realistic approach for cartilage (Li et al., 1999; Li et al., 2000; Korhonen et al., 2003; Wilson et al., 2004; Wilson et al., 2005b; Julkunen et al., 2007; Korhonen et al., 2008; Julkunen et al., 2009). It should also be noted that in articular cartilage negative fixed charges create tissue swelling pressure and is very important for the mechanical behaviour of the tissue. Thus, tissue swelling model or triphasic approaches are important phenomena. Meniscus, ligaments and tendons have only a small amount of fixed charges and swelling mechanisms have thus been neglected in the models.
Meniscus has been typically modelled as isotropic or transversely isotropic material (Spilker et al., 1992; Meakin et al., 2003; Sweigart et al., 2004; Guess et al., 2010). Poroelastic properties have also been included in meniscus models. Typical models for ligaments and tendons have been transversely isotropic nonlinear with hyperelastic behaviour (Pena et al.,

2006; Zhang et al., 2008). Also viscoelastic solid models (Thornton et al., 1997) and poroelastic models have been applied for ligaments (Atkinson et al., 1997). However, the fluid-flow dependent viscoeasticity may not be that important in ligaments and tendons because they experience mainly tensile forces under physiological loading and it has been suggested that fluid has only a minor role in contributing to soft tissue response in tension (Li et al., 2005). Furthermore, viscoelastic models with anisotropic nonlinear stress-strain behaviour have been developed to capture the strain rate dependent nonlinearity of ligaments and tendons (Pioletti et al., 1998; Limbert&Middleton, 2006).

3.7 Optimization of material parameters

The optimization of material parameters of the model can be done by typically minimizing the mean squared error (MSE), root mean squared error (RMSE) or mean absolute error (MAE) between the simulated and experimental force curves (Fig. 5). This can be done for instance using a multidimensional unconstrained nonlinear minimization routine (fminsearch) available in Matlab (Mathworks Inc., Natick, MA, USA). The optimization should be first tested with different initial values of the material parameters, and the optimized parameter values should be always the same, independent on the initial guess. Then one of the equations for MSE, RMSE and MAE,

$$MSE = \frac{1}{n}\sum_{j=1}^{n}\left(F_{model,j} - F_{exp,j}\right)^2, \tag{3.39}$$

$$RMSE = \frac{1}{n}\sum_{j=1}^{n}\sqrt{\left(F_{model,j} - F_{exp,j}\right)^2}, \tag{3.40}$$

$$MAE = \frac{1}{n}\sum_{j=1}^{n}\left|F_{model,j} - F_{exp,j}\right|, \tag{3.41}$$

where $F_{model,j}$ is the model output and $F_{exp,j}$ is the experimental result at any time point (j), can be applied. The optimizations have also been conducted using normalized MSE, RMSE and MAE, i.e. by dividing equations 3.39-3.41 with $F_{exp,j}$ at each time point.

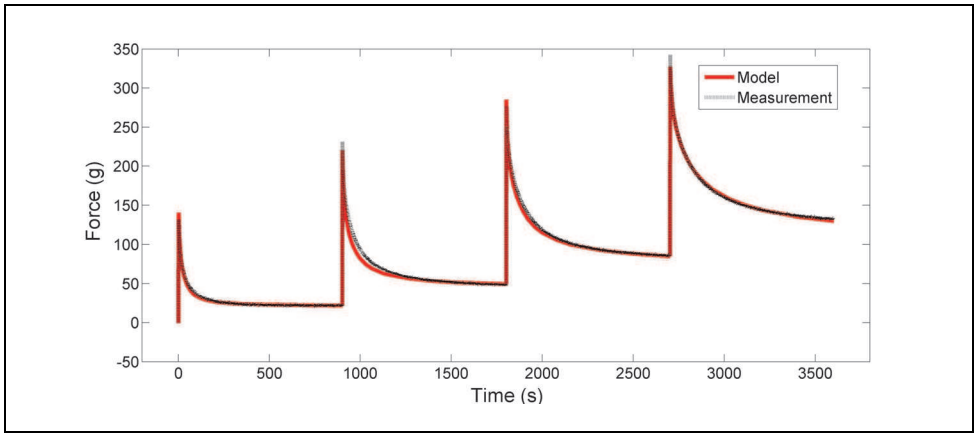

Fig. 5. A typical stress-relaxation measurement of articular cartilage and corresponding optimized model fit using a fibril reinforced poroviscoelastic model.

4. References

Arokoski, J. P., Hyttinen, M. M., Lapveteläinen, T., Takacs, P., Kosztaczky, B., Modis, L., Kovanen, V., Helminen, H., (1996). Decreased birefringence of the superficial zone collagen network in the canine knee (stifle) articular cartilage after long distance running training, detected by quantitative polarised light microscopy. *Ann Rheum Dis* 55, 253-264.

Atkinson, T. S., Haut, R. C., Altiero, N. J., (1997). A poroelastic model that predicts some phenomenological responses of ligaments and tendons. *J Biomech Eng* 119, 400-405.

Benninghoff, A., (1925). Form und bau der gelenkknorpel in ihren beziehungen zur function. *Zeitschrift fur Zellforschung* 2, 783-862.

Chen, A. C., Bae, W. C., Schinagl, R. M., Sah, R. L., (2001). Depth- and strain-dependent mechanical and electromechanical properties of full-thickness bovine articular cartilage in confined compression. *J Biomech* 34, 1-12.

Cui, J. H., Min, B. H., (2007). Collagenous fibril texture of the discoid lateral meniscus. *Arthroscopy* 23, 635-641.

DiSilvestro, M. R., Suh, J. K., (2001). A cross-validation of the biphasic poroviscoelastic model of articular cartilage in unconfined compression, indentation, and confined compression. *J Biomech* 34, 519-525.

Elliott, D. M., Narmoneva, D. A., Setton, L. A., (2002). Direct measurement of the Poisson's ratio of human patella cartilage in tension. *J Biomech Eng* 124, 223-228.

Fung, Y. C., (2004). Biomechanics-Mechanical properties of living tissues, second edition. Springer, New York.

Garcia, J. J., Altiero, N. J., Haut, R. C., (2000). Estimation of in situ elastic properties of biphasic cartilage based on a transversely isotropic hypo-elastic model. *J Biomech Eng* 122, 1-8.

Guess, T. M., Thiagarajan, G., Kia, M., Mishra, M., (2010). A subject specific multibody model of the knee with menisci. *Med Eng Phys* 32, 505-515.

Guilak, F., Mow, V. C., (2000). The mechanical environment of the chondrocyte: a biphasic finite element model of cell-matrix interactions in articular cartilage. *J Biomech* 33, 1663-1673.

Hewitt, J., Guilak, F., Glisson, R., Vail, T. P., (2001). Regional material properties of human hip joint capsule ligaments. *J Orthop Res* 19, 359-364.

Huyghe, J. M., Janssen, J. D., (1997). Quadriphasic theory of swelling incompressible porous media. *Int J Eng Sci* 35, 793-802.

Julkunen, P., Kiviranta, P., Wilson, W., Jurvelin, J. S., Korhonen, R. K., (2007). Characterization of articular cartilage by combining microscopic analysis with a fibril-reinforced finite element model. *J Biomech* 40, 1862-1870.

Julkunen, P., Wilson, W., Jurvelin, J. S., Korhonen, R. K., (2009). Composition of the pericellular matrix modulates the deformation behaviour of chondrocytes in articular cartilage under static loading. *Med Biol Eng Comput* 47, 1281-1290.

Julkunen, P., Wilson, W., Jurvelin, J. S., Rieppo, J., Qu, C. J., Lammi, M. J., Korhonen, R. K., (2008). Stress-relaxation of human patellar articular cartilage in unconfined

compression: prediction of mechanical response by tissue composition and structure. *J Biomech* 41, 1978-1986.

Jurvelin, J. S., Buschmann, M. D., Hunziker, E. B., (1997). Optical and mechanical determination of Poisson's ratio of adult bovine humeral articular cartilage. *J Biomech* 30, 235-241.

Kaab, M. J., Richards, R. G., Ito, K., ap Gwynn, I., Notzli, H. P., (2003). Deformation of chondrocytes in articular cartilage under compressive load: a morphological study. *Cells Tissues Organs* 175, 133-139.

Korhonen, R. K., Julkunen, P., Wilson, W., Herzog, W., (2008). Importance of collagen orientation and depth-dependent fixed charge densities of cartilage on mechanical behavior of chondrocytes. *J Biomech Eng* 130, 021003.

Korhonen, R. K., Laasanen, M. S., Toyras, J., Lappalainen, R., Helminen, H. J., Jurvelin, J. S., (2003). Fibril reinforced poroelastic model predicts specifically mechanical behavior of normal, proteoglycan depleted and collagen degraded articular cartilage. *J Biomech* 36, 1373-1379.

Korhonen, R. K., Laasanen, M. S., Töyräs, J., Helminen, H. J., Jurvelin, J. S., (2002a). Comparison of the equilibrium response of articular cartilage in unconfined compression, confined compression and indentation. *J Biomech* 35, 903-909.

Korhonen, R. K., Wong, M., Arokoski, J., Lindgren, R., Helminen, H. J., Hunziker, E. B., Jurvelin, J. S., (2002b). Importance of the superficial tissue layer for the indentation stiffness of articular cartilage. *Med Eng Phys* 24, 99-108.

Laasanen, M. S., Toyras, J., Korhonen, R. K., Rieppo, J., Saarakkala, S., Nieminen, M. T., Hirvonen, J., Jurvelin, J. S., (2003). Biomechanical properties of knee articular cartilage. *Biorheology* 40, 133-140.

Lai, W. M., Hou, J. S., Mow, V. C., (1991). A triphasic theory for the swelling and deformation behaviors of articular cartilage. *J Biomech Eng* 113, 245-258.

Li, L. P., Buschmann, M. D., Shirazi-Adl, A., (2000). A fibril reinforced nonhomogeneous poroelastic model for articular cartilage: inhomogeneous response in unconfined compression. *J Biomech* 33, 1533-1541.

Li, L. P., Herzog, W., Korhonen, R. K., Jurvelin, J. S., (2005). The role of viscoelasticity of collagen fibers in articular cartilage: axial tension versus compression. *Med Eng Phys* 27, 51-57.

Li, L. P., Soulhat, J., Buschmann, M. D., Shirazi-Adl, A., (1999). Nonlinear analysis of cartilage in unconfined ramp compression using a fibril reinforced poroelastic model. *Clin Biomech* 14, 673-682.

Limbert, G., Middleton, J., (2006). A constitutive model of the posterior cruciate ligament. *Med Eng Phys* 28, 99-113.

Maroudas, A., (1968). Physicochemical properties of cartilage in the light of ion exchange theory. *Biophys J* 8, 575-595.

McDevitt, C. A., Webber, R. J., (1990). The ultrastructure and biochemistry of meniscal cartilage. *Clin Orthop*, 8-18.

Meakin, J. R., Shrive, N. G., Frank, C. B., Hart, D. A., (2003). Finite element analysis of the meniscus: the influence of geometry and material properties on its behaviour. *Knee* 10, 33-41.

Messner, K., Gao, J., (1998). The menisci of the knee joint. Anatomical and functional characteristics, and a rationale for clinical treatment. *J Anat* 193, 161-178.

Mow, V. C., Gu, W. Y., Chen, F. H., (2005). Structure and function of articular cartilage and meniscus. In: Mow, V. C., Huiskes, R. (Eds.), *Basic Orthopaedic Biomechanics and Mechano-biology*. Lippincott Williams & Wilkins, Philadelphia, pp. 181-258.

Mow, V. C., Kuei, S. C., Lai, W. M., Armstrong, C. G., (1980). Biphasic creep and stress relaxation of articular cartilage in compression: Theory and experiments. *J Biomech Eng* 102, 73-84.

Pena, E., Calvo, B., Martinez, M. A., Doblare, M., (2006). A three-dimensional finite element analysis of the combined behavior of ligaments and menisci in the healthy human knee joint. *J Biomech* 39, 1686-1701.

Pioletti, D. P., Rakotomanana, L. R., Benvenuti, J. F., Leyvraz, P. F., (1998). Viscoelastic constitutive law in large deformations: application to human knee ligaments and tendons. *J Biomech* 31, 753-757.

Soltz, M. A., Ateshian, G. A., (2000). A Conewise Linear Elasticity mixture model for the analysis of tension- compression nonlinearity in articular cartilage. *J Biomech Eng* 122, 576-586.

Spilker, R. L., Donzelli, P. S., Mow, V. C., (1992). A transversely isotropic biphasic finite element model of the meniscus. *J Biomech* 25, 1027-1045.

Sweigart, M. A., Zhu, C. F., Burt, D. M., DeHoll, P. D., Agrawal, C. M., Clanton, T. O., Athanasiou, K. A., (2004). Intraspecies and interspecies comparison of the compressive properties of the medial meniscus. *Ann Biomed Eng* 32, 1569-1579.

Thornton, G. M., Oliynyk, A., Frank, C. B., Shrive, N. G., (1997). Ligament creep cannot be predicted from stress relaxation at low stress: a biomechanical study of the rabbit medial collateral ligament. *J Orthop Res* 15, 652-656.

Vasara, A. I., Jurvelin, J. S., Peterson, L., Kiviranta, I., (2005). Arthroscopic cartilage indentation and cartilage lesions of anterior cruciate ligament-deficient knees. *Am J Sports Med* 33, 408-414.

Wilson, W., Huyghe, J. M., van Donkelaar, C. C., (2006). A composition-based cartilage model for the assessment of compositional changes during cartilage damage and adaptation. *Osteoarthritis Cartilage* 14, 554-560.

Wilson, W., van Donkelaar, C. C., Huyghe, J. M., (2005a). A comparison between mechano-electrochemical and biphasic swelling theories for soft hydrated tissues. *J Biomech Eng* 127, 158-165.

Wilson, W., van Donkelaar, C. C., van Rietbergen, B., Huiskes, R., (2005b). A fibril-reinforced poroviscoelastic swelling model for articular cartilage. *J Biomech* 38, 1195-1204.

Wilson, W., van Donkelaar, C. C., van Rietbergen, B., Ito, K., Huiskes, R., (2004). Stresses in the local collagen network of articular cartilage: a poroviscoelastic fibril-reinforced finite element study. *J Biomech* 37, 357-366.

Woo, S. L., Lee, T. Q., Abramowitch, S. D., Gilbert, T. W., (2005). Structure and function of ligaments and tendons. In: Mow, V. C., Huiskes, R. (Eds.), *Basic Orthopaedic Biomechanics and Mechano-biology*. Lippincott Williams & Wilkins, Philadelphia, pp. 301-342.

Zhang, X., Jiang, G., Wu, C., Woo, S. L., (2008). A subject-specific finite element model of the anterior cruciate ligament. In *30th Annual International Conference of the IEEE Engineering in Medicine & Biology Society*. Vancouver, British Columbia, Canada, August 20-24, pp. 891-894.

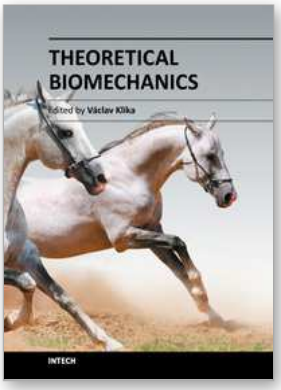

Theoretical Biomechanics

Edited by Dr Vaclav Klika

ISBN 978-953-307-851-9
Hard cover, 402 pages
Publisher InTech
Published online 25, November, 2011
Published in print edition November, 2011

During last couple of years there has been an increasing recognition that problems arising in biology or related to medicine really need a multidisciplinary approach. For this reason some special branches of both applied theoretical physics and mathematics have recently emerged such as biomechanics, mechanobiology, mathematical biology, biothermodynamics. This first section of the book, General notes on biomechanics and mechanobiology, comprises from theoretical contributions to Biomechanics often providing hypothesis or rationale for a given phenomenon that experiment or clinical study cannot provide. It deals with mechanical properties of living cells and tissues, mechanobiology of fracture healing or evolution of locomotor trends in extinct terrestrial giants. The second section, Biomechanical modelling, is devoted to the rapidly growing field of biomechanical models and modelling approaches to improve our understanding about processes in human body. The last section called Locomotion and joint biomechanics is a collection of works on description and analysis of human locomotion, joint stability and acting forces.

How to reference

In order to correctly reference this scholarly work, feel free to copy and paste the following:

Rami K. Korhonen and Simo Saarakkala (2011). Biomechanics and Modeling of Skeletal Soft Tissues, Theoretical Biomechanics, Dr Vaclav Klika (Ed.), ISBN: 978-953-307-851-9, InTech, Available from: http://www.intechopen.com/books/theoretical-biomechanics/biomechanics-and-modeling-of-skeletal-soft-tissues

INTECH
open science | open minds

InTech Europe
University Campus STeP Ri
Slavka Krautzeka 83/A
51000 Rijeka, Croatia
Phone: +385 (51) 770 447
Fax: +385 (51) 686 166
www.intechopen.com

InTech China
Unit 405, Office Block, Hotel Equatorial Shanghai
No.65, Yan An Road (West), Shanghai, 200040, China
中国上海市延安西路65号上海国际贵都大饭店办公楼405单元
Phone: +86-21-62489820
Fax: +86-21-62489821